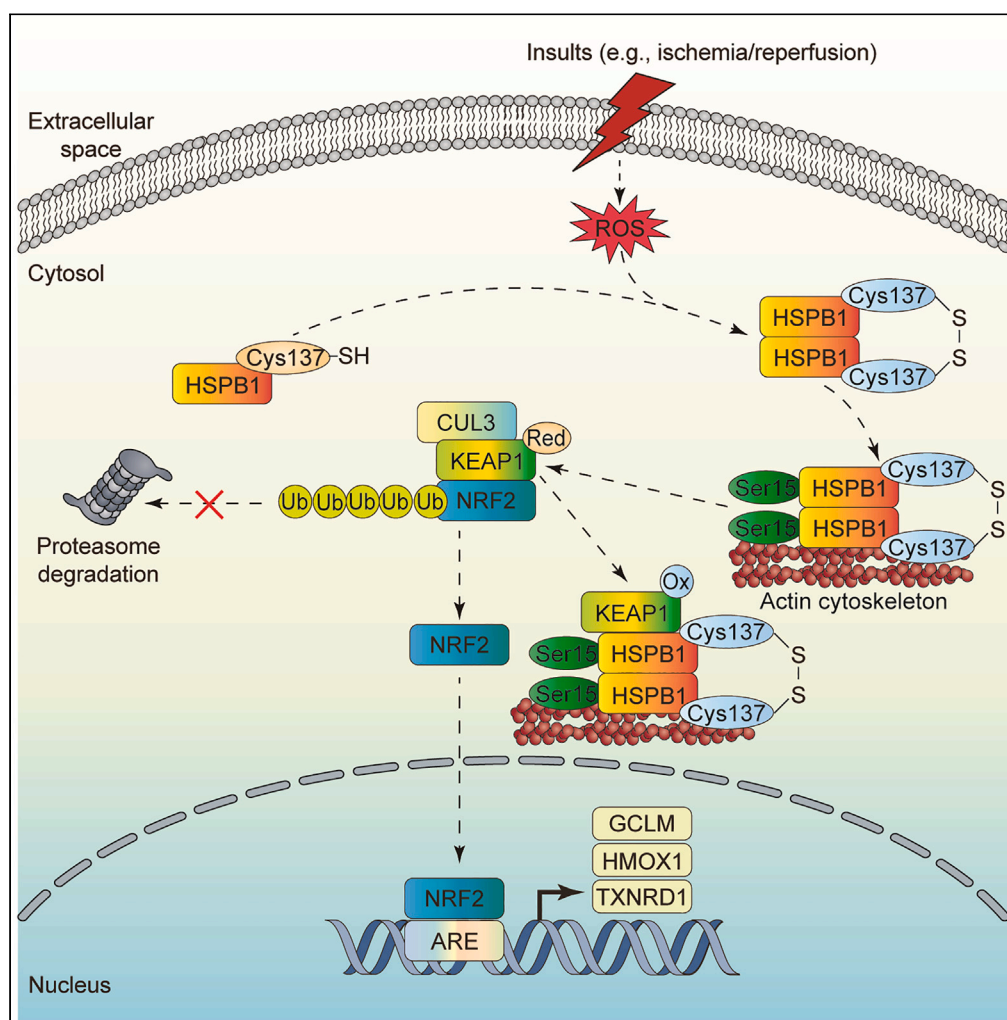**Article**

Homo-oxidized HSPB1 protects H9c2 cells against oxidative stress via activation of KEAP1/NRF2 signaling pathway

Nian Wang,
Xiehong Liu, Ke
Liu, Kangkai
Wang, Huali
Zhang

wangkangkai@csu.edu.cn
(K.W.)
zhanghuali@csu.edu.cn (H.Z.)

Highlights
Homo-oxidized HSPB1
forms in the
cardiomyocytes
undergoing oxidative
stress

Cys137 is required for
HSPB1 to protect
cardiomyocytes against
oxidative injury

Cys137 is indispensable
for HSPB1 to interact with
KEAP1 following oxidative
stress

Article

Homo-oxidized HSPB1 protects H9c2 cells against oxidative stress via activation of KEAP1/NRF2 signaling pathway

Nian Wang,[1,2,3] Xiehong Liu,[1,2,3] Ke Liu,[1,2,3] Kangkai Wang,[1,2,3,*] and Huali Zhang[1,2,3,4,*]

SUMMARY

Several heat shock proteins are implicated in the endogenous cardioprotective mechanisms, but little is known about the role of heat shock protein beta-1 (HSPB1). This study aims to investigate the oxidation state and role of HSPB1 in cardiomyocytes undergoing oxidative stress and underlying mechanisms. Here, we demonstrate that hydrogen peroxide (H_2O_2) promotes the homo-oxidation of HSPB1. Cys137 residue of HSPB1 is not only required for it to protect cardiomyocytes against oxidative injury but also modulates its oxidation, phosphorylation at Ser15, and distribution to insoluble cell components after H_2O_2 treatment. Moreover, Cys137 residue is indispensable for HSPB1 to interact with KEAP1, thus regulating its oxidation and intracellular distribution, subsequently promoting the nuclear translocation of NRF2, and increasing the transcription of *GLCM*, *HMOX1*, and *TXNRD1*. Altogether, these findings provide evidence that Cys137 residue is indispensable for HSPB1 to maintain its redox state and antioxidant activity via activating KEAP1/NRF2 signaling cascade in cardiomyocytes.

INTRODUCTION

Myocardial ischemia, a clinical phenomenon that describes a set of conditions known as ischemic heart disease, is characterized by the imbalance between myocardial blood supply and demand. Myocardial infarction (MI) which refers to severe ischemia-induced myocardial necrosis has emerged as one of the most common causes of crippling diseases and death globally.[1,2] Since poor perfusion is the primary pathophysiologic defect following ischemia, MI is associated with inadequate oxygen delivery and nutrition supply as well as accumulation of metabolic waste products in the myocardium. Therefore, oxidative stress is involved in the pathogenic process of myocardial ischemia, and it is essential for the cascade progression of myocardial ischemia-reperfusion injury.[3,4]

Oxidative stress is considered as a disequilibrium between reactive oxygen species (ROS) production and endogenous antioxidative machinery, namely "redox state". Excessive ROS can result in cell malfunction through damaging lipids, proteins, and DNA, ultimately causes irreversible cell damage and death. To counteract increasing ROS generation induced by noxious stimuli, several endogenous antioxidative machinery that are grouped as enzymatic and non-enzymatic antioxidant systems are evolved in cells. Antioxidant enzymes systems are mainly consisted of superoxide dismutase, glutathione peroxidase, and catalase, while non-enzymatic antioxidants include glutathione (GSH), melatonin, uric acid, vitamins A, E, and C, etc.[5–7] In addition, heat shock proteins (HSPs) are produced in response to oxidative stress and interact closely with the antioxidant systems through regulation of various redox processes.[8] There has been mounting evidence that HSPs exhibit distinguished cytoprotective effects against oxidative stress-induced ischemic myocardial injury.[9–11] However, the roles and mechanisms of small HSPs in oxidative myocardial injury remain largely unknown.

Small HSPs represent a class of molecular chaperones that are involved in maintaining the redox homeostasis through upholding the level of GSH, and thus serve as a first line of defense against various stress-induced cell damage. To date, 10 kinds of small HSPs have been identified in humans (HSPB1-10), in which heat shock protein beta-1 (HSPB1) and HSPB5 have high constitutive levels in the heart and are stress inducible.[12] HSPB1 can exert strong antioxidant activities through maintaining the levels of reduced GSH and

[1]Department of Pathophysiology, School of Basic Medicine Science, Central South University, Changsha, China

[2]Sepsis Translational Medicine Key Laboratory of Hunan Province, Central South University, Changsha, Hunan 410078, P.R. China

[3]National Medicine Functional Experimental Teaching Center, Central South University, Changsha, Hunan 410078, P.R. China

[4]Lead contact

*Correspondence: wangkangkai@csu.edu.cn (K.W.), zhanghuali@csu.edu.cn (H.Z.) https://doi.org/10.1016/j.isci.2023.107443

stabilizing mitochondrial membrane.[13,14] Our previous studies show that HSPB1 not only regulates the reduced state of endogenous antioxidant pathways in H9c2 cells under oxidative stress but also maintains the redox state of cytoplasm via modulation of Hippo-Yes-associated protein 1 signaling pathway. Consequently, HSPB1 inhibits the oxidation of proteins, reduces DNA damage and lipid peroxidation, and stabilizes the actin cytoskeleton of cardiomyocytes.[15] It has been proved that HSPB1 is a redox-sensitive molecular chaperone, and its expression is upregulated under different stress conditions including oxidative stress, which is accompanied by partial oxidation of its single cysteine (Cys) residue and formation of cross-linked dimer.[16,17] Oxidation affects the stability and conformational mobility of HSPB1 and contributes to the decrease of its molecular chaperone activity.[18] However, the redox state of HSPB1 in the cardiomyocytes undergoing oxidative stress has not been well defined. Moreover, little is known about the downstream effect regulated by the redox state of HSPB1 in cardiomyocytes undergoing oxidative stress.

Kelch-like ECH-associated protein 1/nuclear factor (erythroid-derived 2)-like 2 (KEAP/NRF2), a redox-sensitive signaling pathway, serves a pivotal role in protecting cells against oxidative injury through regulating the transcription of antioxidant and detoxification genes.[19,20] Compelling evidence indicates that aberrant KEAP1/NRF2 signaling is implicated in various myocardial injury, such as myocardial ischemia-reperfusion injury, pathological cardiac hypertrophy, and cisplatin-induced cardiotoxicity.[21–23] Although the crosstalk between HSPs and KEAP1/NRF2 signaling has been addressed in the early neonatal unilateral ureteral obstruction, inflammation, and oxidative injury in airway epithelial cells,[24–26] what we have known is just a tip of the iceberg. The interaction between HSPB1 and KEAP1/NRF2 signaling upon oxidative stress has not yet been fully elucidated.

Based on our previous studies, this study was designed to define the redox state of HSPB1 in cardiomyocytes undergoing oxidative stress, determine the role of oxidized HSPB1 in oxidative myocardial injury, and clarify the potential molecular mechanisms underlying its oxidative activities.

RESULTS

Homo-oxidized HSPB1 forms in the H9c2 cells under oxidative stress condition

To clarify the effect of oxidative stress on the redox state of HSPB1, different doses of H_2O_2 were used to treat rat H9c2 cardiomyocytes for 30 min, non-reducing western blotting showed that H_2O_2 increased the expression of both oxidized and reduced HSPB1 in a dose-dependent manner, and 0.75 mM H_2O_2 induced a maximum production of oxidized HSPB1 (Figures 1A–1C). Further, time course analysis showed that maximum production of oxidized HSPB1 reached at 15 min following H_2O_2 challenge. Meanwhile, H_2O_2 decreased expression of reduced HSPB1 in a time-dependent manner (Figures 1D–1F). NAC, a reduced glutathione precursor, can protect against oxidative injury through breaking thiolated proteins and releasing free thiols as well as reduced proteins.[27] To further identify the formation of oxidized HSPB1 under oxidative stress conditions, H9c2 cells were pretreated by NAC for 1 h and then subjected to H_2O_2. It was found that NAC could block the formation of oxidized HSPB1 at 30 min after H_2O_2 challenge (Figures 1G and 1H). These data indicated that H_2O_2 could promote the formation of oxidized HSPB1.

As a ubiquitously expressed molecular chaperone, HSPB1 could form homologous oxidized HSPB1 (homo-oxidized HSPB1) through S-thiolated modification of its own unique cysteine, and thus exerted antioxidant activities.[28,29] To identify whether oxidative stress could induce the formation of homo-oxidized HSPB1 in cardiomyocytes, HSPB1 short interfering RNA (siRNA) was used to knock down the expression of endogenous HSPB1 in H9c2 cells, and then exogenous human HSPB1 was expressed in H9c2 cells through transfection with pCMV-myc-HSPB1 and/or pCMV-HA-HSPB1. In the absence of beta-mercaptoethanol (BME), non-reducing blotting showed that H_2O_2 challenge promoted the formation of oxidized HSPB1 in H9c2 cells that exogenously expressed human HSPB1 (Figure 1I, upper panel). However, no formation of oxidized HSPB1 was observed in the presence of BME using reducing western blotting (Figure 1I, lower panel). Furthermore, when H9c2 cells were co-transfected with pCMV-myc-HSPB1 and pCMV-HA-HSPB1 plasmids and exposed to H_2O_2, exogenously expressed HSPB1 could be detected using anti-MYC antibody in the complex that was immunoprecipitated by anti-HA-tag antibody (Figure 1I). Altogether, these data indicated that homo-oxidized HSPB1 formed in rat H9c2 cardiomyocytes during oxidative stress.

Cys137 residue is required for HSPB1 to protect H9c2 cells against oxidative injury

Among ten kinds of human heat shock proteins, HSPB1 is unique because it contains a single cysteine residue (Cys137) that locates in the β7 strand of its α-crystallin domain. Cys137 residue has been proved to be
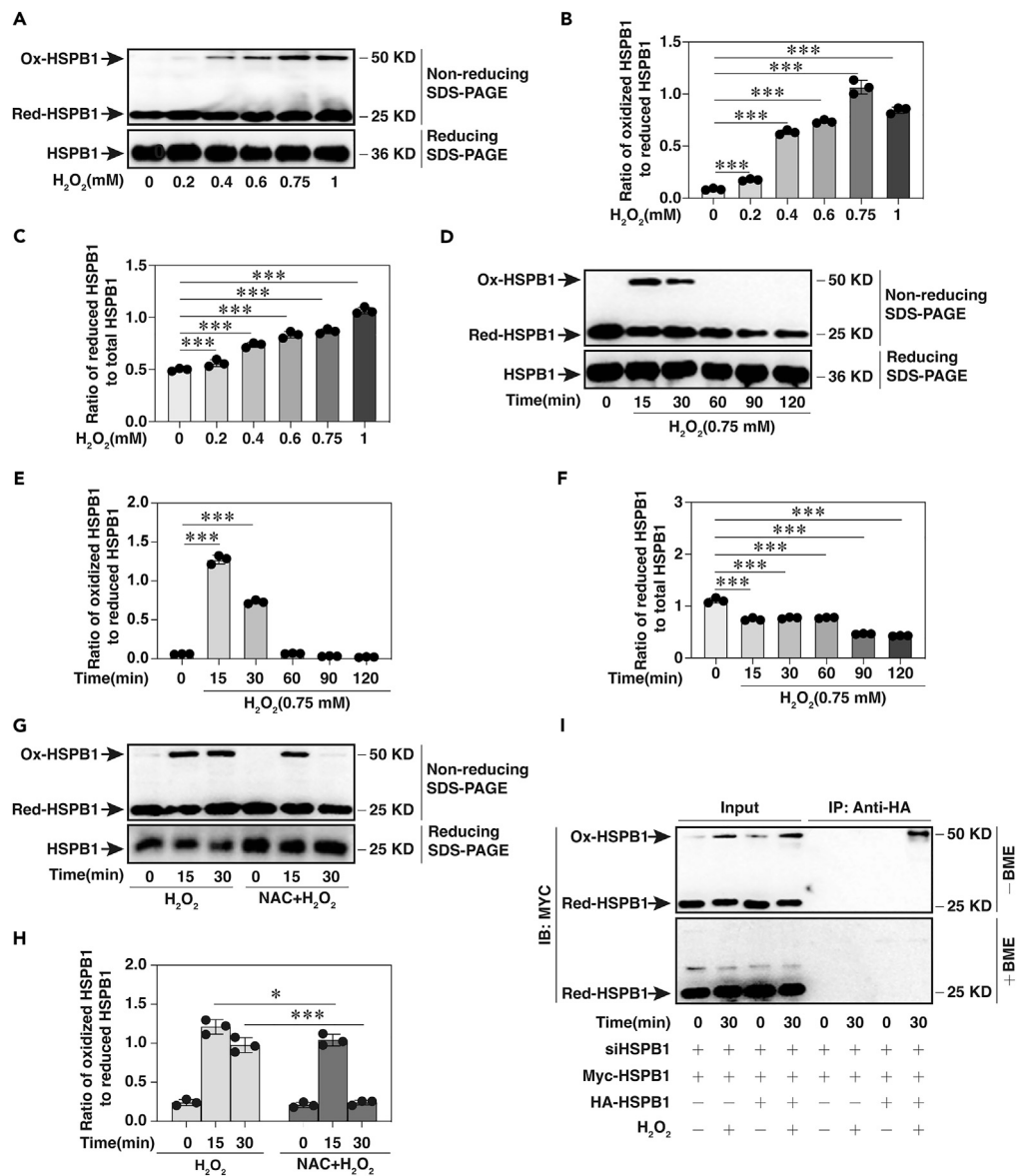
Figure 1. Homo-oxidized HSPB1 formed in rat H9c2 cardiomyocytes exposed to H_2O_2

(A) H9c2 cells were treated by different doses of H_2O_2 (0.2, 0.4, 0.75, and 1 mM) for 30 min. The expression of oxidized and reduced HSPB1 was detected by NEM-alkylated redox-western blotting (non-reducing western blotting), while the expression of total HSPB1 was determined by reducing western blotting.

(B and C) Accordingly, the relative expression of oxidized and reduced HSPB1 was quantified by densitometry analysis of bands. Histogram showed the ratio of oxidized HSPB1 to reduced HSPB1 (B) and the ratio of reduced HSPB1 to total HSPB1 expression (C).

(D) H9c2 cells were treated by 0.75 mM H_2O_2 for different time. The expression of oxidized and reduced HSPB1 as well as HSPB1 was detected as described above.

(E and F) Accordingly, the relative expression of oxidized and reduced HSPB1 was quantified by densitometry analysis of bands. Histogram showed the ratio of oxidized HSPB1 to reduced HSPB1 (E) and the ratio of reduced HSPB1 to total HSPB1 expression (F).

(G) H9c2 cells were pretreatment with 0.4 mM NAC for 1 h, and then the cells were treated with 0.75 mM of H_2O_2 for 30 min. The expression of oxidized and reduced HSPB1 as well as HSP1 was detected as described above.

(H) Accordingly, the relative expression of oxidized and reduced HSPB1 was quantified by densitometry analysis of bands. Histogram showed the ratio of oxidized HSPB1 to reduced HSPB1.

existed in either its oxidized (disulfide) or reduced (thiol) form and is essential for the function of HSPB1.[30] To identify whether Cys137 residue mediates the redox state of HSP1B under oxidative stress, site-directed mutagenesis of TGT (Cys137) to AGC (Ser137) was carried out in pCMV-Myc-HSPB1 plasmid, i.e., pCMV-Myc-HSPB1-C137S. No detectable band indicating oxidized HSP1B was observed in H_2O_2-treated H9c2 cells transfected with pCMV-Myc-HSPB1-C137S (Figure 2A). These results suggested that Cys137 residue was required for the formation of oxidized HSPB1 in cardiomyocytes upon oxidative stress. In addition, transfection with pCMV-Myc-HSPB1 not only elevated the cell viability but also reduced the activities of caspase-3 (CASP3), caspase-8 (CASP8), and caspase-9 (CASP9) in H9c2 cells. On the contrary, transfection with pCMV-Myc-HSPB1-C137S resulted in lower cell viability and higher activities of CASP3, CASP8, and CASP9 in H9c2 cells with or without H_2O_2 treatment (Figures 2B–2E). Furthermore, knockdown of HSPB1 using specific siHSPB1 obviously increased the apoptotic rate of H9c2 cells in the presence or absence of H_2O_2, and co-transfection with pCMV-Myc-HSPB1 abrogated the pro-apoptotic effect of siHSPB1. However, co-transfection with pCMV-Myc-HSPB1-C137S failed to elicit a discernible improvement that was similar as pCMV-Myc-HSPB1 (Figures 2F–2H). These results suggested that Cys137 residue was required for HSPB1 to maintain its redox state and protect cardiomyocytes against oxidative injury.

Cys137 residue of HSPB1 modulates its phosphorylation at Ser15 and distribution to insoluble components in the H9c2 cells upon oxidative stress

HSPB1 was originally known as a phosphoprotein; it was characterized by dynamic phosphorylation leading to heterogeneous oligomerization under various pathological conditions.[18,31,32] Phosphorylation affects not only the oligomerization but also the chaperone-like activity of HSPB1. In humans, three phosphorylatable serine sites (Ser15, Ser78, and Ser82) located in the N-terminal part of HSPB1 had been identified, while only two phosphorylatable serine sites (Ser15 and Ser86) had been determined in rat HSPB1.[33,34] To elucidate the role of Cys137 residue in oxidative stress-induced phosphorylation of HSPB1, H9c2 cells were treated by H_2O_2 for different time. Given that H_2O_2 failed to induce Ser86 phosphorylation of HSPB1, the Ser15 phosphorylation of HSPB1 in H9c2 cells peaked after 15 min exposure to H_2O_2, and continuously decreased after 30 min exposure to H_2O_2 (Figures 3A and 3B). Moreover, the Ser15 phosphorylation of HSPB1 was increased in H9c2 cells that overexpressed exogenous human HSPB1 but decreased in H9c2 cells that overexpressed exogenous human HSPB1 with Cys137 mutation in the presence or absence of H_2O_2 (Figures 3C and 3D). Meanwhile, overexpression of human HSPB1 with Cys137 mutation failed to influence H_2O_2-induced Ser78 phosphorylation in H9c2 cells (Figure 3C). These data indicated that Cys137 residue was required for the phosphorylation of HSPB1 at Ser15, which might be uniquely important for the biological activity of HSPB1.

Under basal conditions, HSPB1 was mainly found in the soluble cytosolic protein fractions by its unphosphorylated form. After being phosphorylated in response to different stimuli or disease states, a conformational change of HSPB1 occurred from the monomer to a wide range of oligomers, and thus more HSPB1 could be found in the insoluble cytoskeletal fractions.[35–38] Indeed, distribution of HSPB1 increased in the insoluble cellular fractions but decreased in the soluble cellular fractions from H9c2 cells with or without exogenous overexpression of wild-type human HSPB1 with the time of H_2O_2 exposure (Figures 3E, 3F, and S1). However, HSPB1 was predominantly found in the soluble cellular fractions from H9c2 cells that overexpressed exogenous human HSPB1 with Cys137 mutation in the presence or absence of H_2O_2 (Figures 3F–3H). These data further suggested that Cys137 residue was responsible for HSPB1 to redistribute to insoluble cytoskeletal fraction and bind to its client proteins in the cardiomyocytes upon oxidative stress.

Cys137 residue is indispensable for HSPB1 to interact with KEAP1 and regulates the oxidation of KEAP1 in the H9c2 cells under oxidative stress

While KEAP-NRF2 signaling pathway played an essential role in protecting cells against oxidative stress, the correlation between HSPB1 and KEAP1-NRF2 signaling during oxidative stress remained obscure.
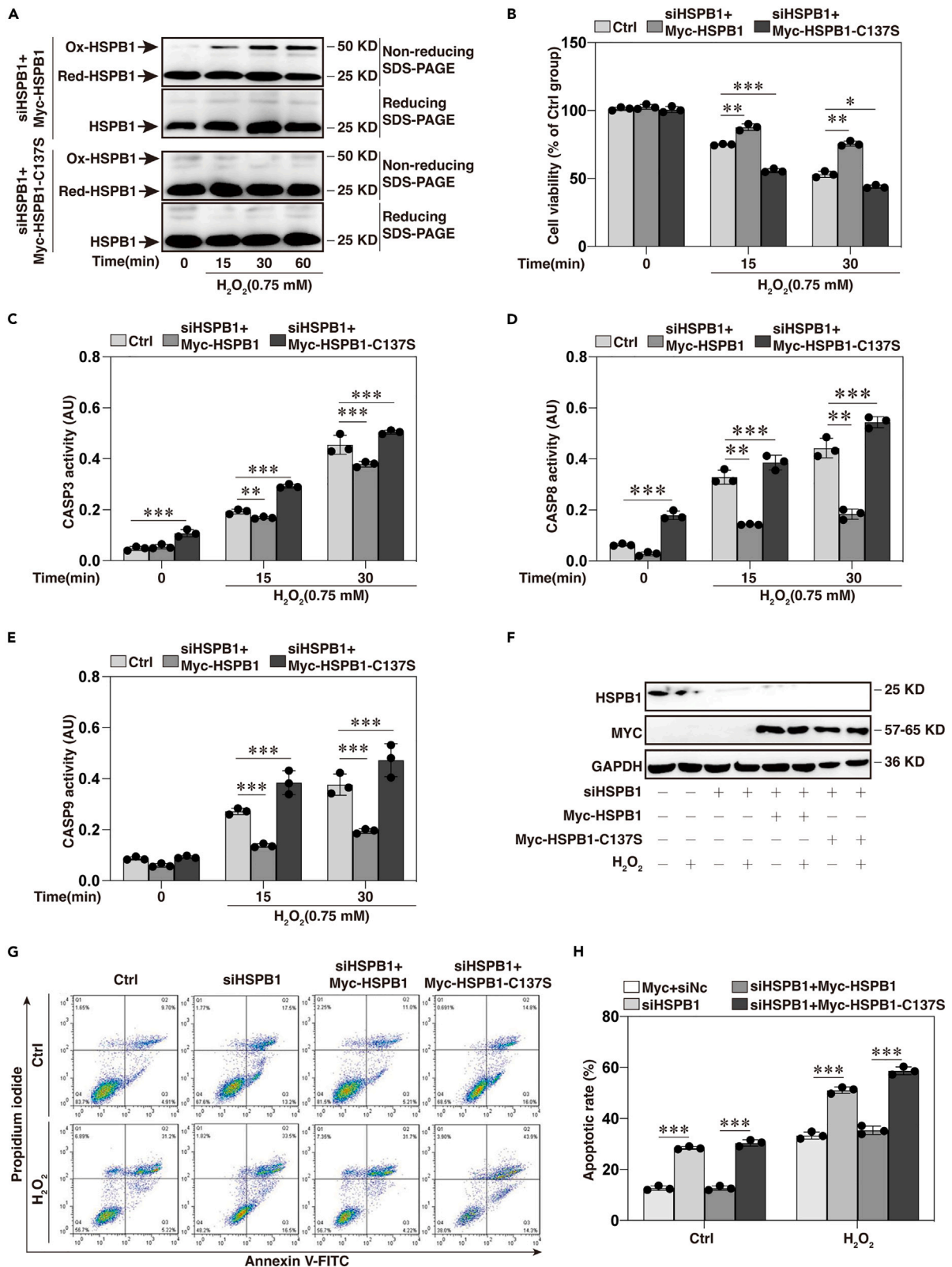
Figure 2. Mutation of HSPB1 in Cys137 exacerbated H_2O_2-induced apoptosis in rat H9c2 cardiomyocytes

(A) H9c2 cells were transfected with pCMV-myc-HSPB1 or pCMV-myc-HSPB1-C137S for 48 h. Subsequently, H9c2 cells were treated with 0.75 mM of H_2O_2 for 15-, 30-, and 60-min. The expression of oxidized and reduced HSPB1 as well as HSP1 was detected as described above.

(B) H9c2 cells were transfected HSPB1 siRNA for 24 h, and then transfected with pCMV-myc-HSPB1 or pCMV-myc-HSPB1-C137S for 48 h. Subsequently, cells were treated with 0.75 mM H_2O_2 for 15- and 30-min. Cell viability was detected by MTT assay.

(C–E) H9c2 cells were transfected HSPB1 siRNA for 24 h, and then transfected with pCMV-myc-HSPB1 or pCMV-myc-HSPB1-C137S for 48 h. Subsequently, cells were treated with 0.75 mM H_2O_2 for 15- and 30-min. The activities of CASP3 (C), CASP8 (D), and CASP9 (E) were determined using colorimetric method.

(F) Determination of the transfection efficiency of HSPB1 siRNA, pCMV-myc-HSPB1, or pCMV-myc-HSPB1-C137S in H9c2 cells exposed to H_2O_2 through reducing western blotting.

(G) H9c2 cells were transfected HSPB1 siRNA for 24 h, and then transfected with pCMV-myc-HSPB1 or pCMV-myc-HSPB1-C137S for 48 h. Subsequently, cells were treated with 0.75 mM H_2O_2 for 12 h. Apoptotic rate of H9c2 cells was determined by using FITC Annexin V and propidium iodide (PI) double staining and flow cytometry analysis.

(H) Histogram of the apoptotic rate. Measurement data were presented as mean $\pm$ SD. Differences among groups were determined by ANOVA and LSD-test or Student's t tests. *$p < 0.05$, **$p < 0.01$, ***$p < 0.001$.

To address this question, the expression and distribution of KEAP1 in H_2O_2-treated H9c2 cells were detected. It was found that H_2O_2 exposure increased KEAP1 expression and promoted its distribution to the insoluble cytoskeletal fractions from H9c2 cells in a time- and dose-dependent manner (Figures 4A–4C). Similar results were observed in H9c2 cells that overexpressed exogenous human HSPB1. However, H_2O_2 exposure primarily increased KEAP1 distribution in the soluble cellular fractions from H9c2 cells that overexpressed exogenous human HSPB1 with Cys137 mutation (Figure 4D). The direct interaction between HSPB1 and KEAP1 was further validated by co-immunoprecipitation analysis. Under basal condition, HSP1 could directly bind to KEAP1 (Figure S2). Following H_2O_2 challenge, increased binding of HSPB1 to KEAP1 was observed with the elevation of KEAP1 expression (Figure S3). Similar results were also observed in H9c2 cells that mainly overexpressed exogenous human HSPB1. Nonetheless, no direct interaction between HSPB1 and KEAP1 was found in H9c2 cells that mainly overexpressed exogenous human HSPB1 with Cys137 mutation in the presence or absence of H_2O_2 (Figure 4E). Furthermore, H_2O_2 treatment enhanced oxidized KEAP1 expression in a time-dependent manner (Figures 4F and 4G); Cys137 mutation in HSPB1 dampened the increase of oxidized KEAP1 induced by H_2O_2 (Figures 4H and 4I). Collectively, these findings demonstrated that Cys137 residue was indispensable for HSPB1 to bind to KEAP1 and regulated the oxidation of KEAP1 in the cardiomyocytes under oxidative stress.

Mutation of HSPB1 in Cys137 dampens the activation of NRF2 following oxidative stress

As a principal negative regulator of NRF2, KEAP1 not only controlled the subcellular distribution of NRF2 but also rapidly degraded NRF2 though proteasome system.[20,39] To further confirm the role of HSPB1/KEAP1 pathway, the expression and activation of NRF2 were detected. It was shown that NRF2 expression increased after 15 min exposure to H_2O_2 and peaked at 60 min (Figure 5A). In addition, the nuclear translocation of NRF2 increased with the exposure time of H_2O_2 (Figure S4). Although mutation of HSPB1 in Cys137 failed to influence the expression of NRF2 in the presence or absence of H_2O_2 (Figure 5A), it abrogated H_2O_2-induced nuclear translocation of NRF2 in H9c2 cells with HSPB1 overexpression (Figures 5B–5F and S4). Meanwhile, the mRNA expression of NRF2 target genes (e.g., glutamate-cysteine ligase modifier subunit [*GCLM*], heme oxygenase 1 [*HMOX1*], thioredoxin reductase 1 [*TXNRD1*]) was increased in H9c2 cells exposed to H_2O_2, which were abolished by knockdown of HSPB1 using specific siRNA. Co-transfection with Myc-HSPB1, but not Myc-HSPB1-C137S, reversed the dampening effect of siHSPB1 on the mRNA expression of *GCLM*, *HMOX1*, and TXNRD1 (Figures 5G–5I). These data provided evidence indicating that Cys137 residue was essential for HSPB1 to regulate oxidative stress-induced activation of NRF2 in the cardiomyocytes.

DISCUSSION

Ischemia and hypoxia cause major changes in cellular redox state, which exerts an essential role in cell survival/death decisions. Unbalanced redox reaction can not only bring in uncontrolled ROS production but also result in excess protein oxidation which is the covalent alteration of a protein caused by either direct reactions with ROS or indirect reactions with secondary oxidative stress by-products.[40] Protein oxidation can result in the loss or gain of enzyme activity, inhibition of protein function, aggregation of protein, increased or decreased susceptibility to proteolysis, etc.[41] Although it is well known that HSPs can be rapidly induced after oxidative stress, little is known about their redox status. HSP60 has been found to be oxidized in human liver cancer cell line HepG2, and is responsible for alcohol-induced cellular injury and hepatocyte growth factor-induced cell migration.[42,43] Oxidation of extracellular HSP70 causes
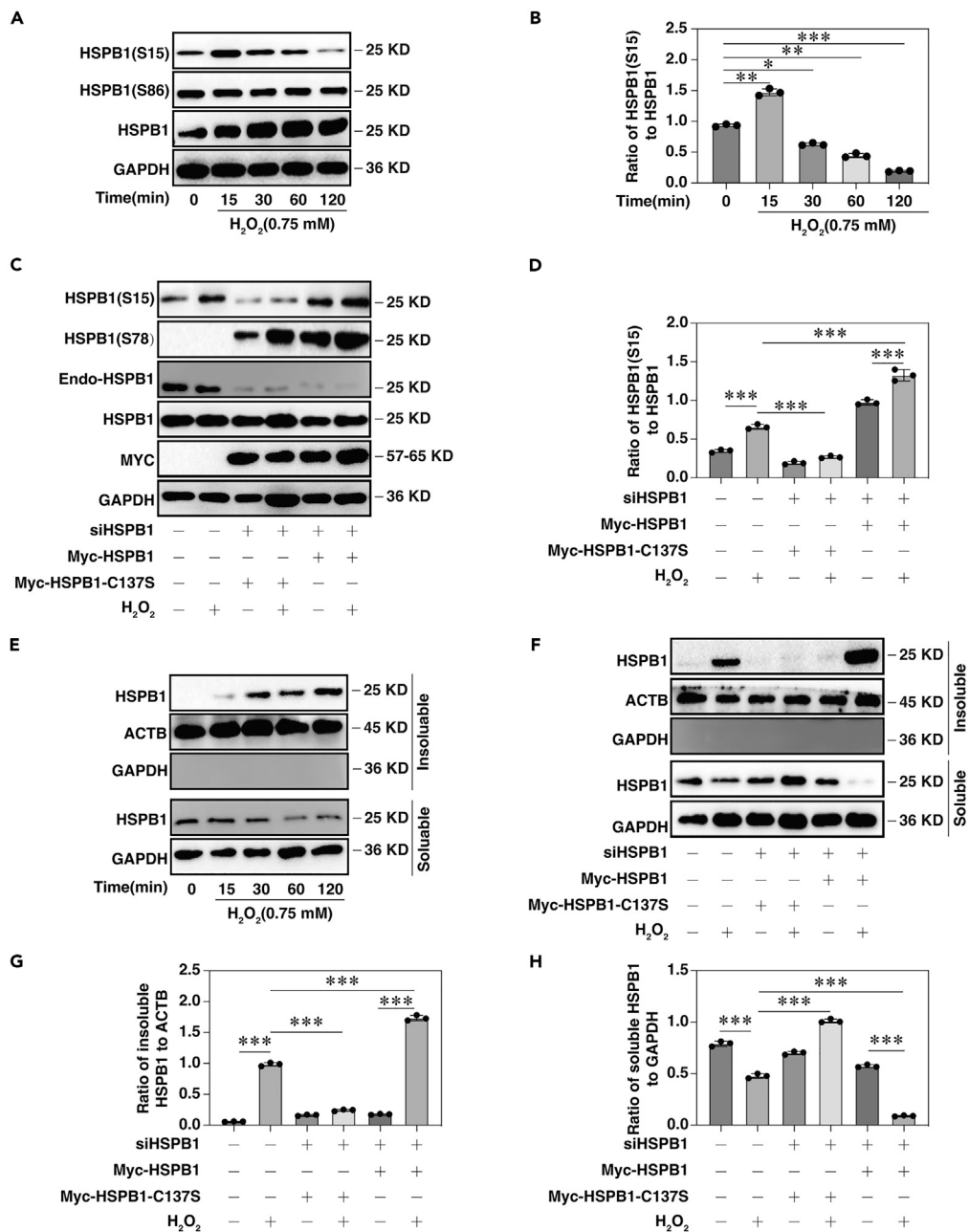
Figure 3. Mutation of HSPB1 in Cys137 inhibited its phosphorylation and distribution to insoluble cell components in rat H9c2 cardiomyocytes exposed to H_2O_2

(A) H9c2 cells were treated with 0.75 mM of H_2O_2 for 15, 30, 60, and 120 min, the expression of phosphorylated HSPB1 and total HSPB1 was detected by reducing western blotting.

(B) Accordingly, histogram shows the ratio of phosphorylated HSPB1 (Ser15) to total HSPB1 expression.

(C) H9c2 cells were transfected HSPB1 siRNA for 24 h, and then transfected with pCMV-myc-HSPB1 or pCMV-myc-HSPB1-C137S for 48 h. Subsequently, cells were treated with or without 0.75 mM H_2O_2 for 30 min. The expression of phosphorylated HSPB1 and total HSPB1 was detected by reducing western blotting.

(D) Accordingly, histogram shows the ratio of phosphorylated HSPB1 (Ser15) to total HSPB1 expression.

(E) H9c2 cells were treated with 0.75 mM of H2O2 for 15, 30, 60, and 120 min, the expression of HSPB1 in soluble and insoluble cell components was detected by reducing western blotting.

Figure 3. *Continued*

(F) H9c2 cells were transfected HSPB1 siRNA for 24 h, and then transfected with pCMV-myc-HSPB1 or pCMV-myc-HSPB1 (C137S) for 48 h. Subsequently, cells were treated with 0.75 mM H_2O_2 for 120 min, the expression of HSPB1 in soluble and insoluble cell components was detected by reducing western blotting.

(G and H) Accordingly, histogram showed the ratio of insoluble HSPB1 to ACTB expression (G) and soluble HSPB1 to GAPDH expression (H). Measurement data were presented as mean ± SD. Differences among groups were determined by ANOVA and LSD-test or Student's t tests. *p < 0.05, **p < 0.01, ***p < 0.001.

functional impairment and inadequate stimulatory capacity of macrophages.[44] In this study, oxidative stress induces the formation of oxidized HSPB1 in the cardiomyocytes, which can be abrogated by NAC pretreatment. Moreover, HSPB1 can be homo-oxidized in this context. Given that HSPB1 regulates oxidative stress-induced apoptosis in cardiomyocytes,[45] these data provide line of evidence indicating that homo-oxidization of HSPB1 may be involved in oxidative myocardial injury.

Like all other sHSP members, HSPB1 also contains a highly conserved core α-crystallin domain (ACD) flanked by a short variable C-terminal region and a longer and flexible N-terminal domain.[46] ACD is responsible for mediating dimer formation of individual protomers, which then can assemble into larger oligomers, while N- and C-terminal domains have propensities to mediate interdimer interactions driving the formation of the sHSP oligomers. Human HSPB1 has sole cysteine residue (C137) located in its ACD, which is highly conserved in HSPB1 orthologs but not found in other mammalian sHSPs, implying that it may play a unique functional role.[16,47] Indeed, HSPB1 is sensitive to the intracellular redox state via its Cys137 residue, which is susceptible to oxidation across the dimer interface, and thus provides structural stability, facilitates the binding of client proteins, regulates the oligomerization of HSPB1, and eventually contributes to the reduction of chaperone-like activity of HSPB1.[17,30,44,47–49] Mutation of C137 residue to A137 in HSPB1 prevents itself to form dimers through disulfide bonds and bind to its client protein CYCS, and thus fails to inhibit the activation of CASP3 and CASP9 and etoposide-induced apoptosis.[50] Murine HSPB1 contains single cysteine residue (Cys141) that is indispensable for itself to form dimers. Polypeptide with C141A mutation exhibits decreased ability to multimerize and no *in vivo* chaperone activity (50). In this study, C137 residue not only determines the redox state of HSPB1 upon oxidative stress but also is required for the HSPB1 to protect cardiomyocytes against oxidative injury. These findings highlight the structural basis (C137 residue) for the antioxidant properties of HSPB1.

It has been proposed that the oligomerization and phosphorylation of HSPB1 is the necessary prerequisites for it to interact with client proteins and exert molecular chaperone activity under oxidative conditions.[51,52] Human HSPB1 possesses three phosphorylatable serine sites (Ser15, Ser78, and Ser82) in the N terminus, while murine HSPB1 has only two phosphorylatable serine sites (Ser15 and Ser86). Previous studies show that Ser78 and/or Ser82 phosphorylation mainly regulate the oligomerization of HSPB1, while Ser15 exhibits little effect on oligomerization.[34,53] In murine cardiomyocyte cell line, Ser15 phosphorylation of HSPB1 is induced by oxidative stress. While both Ser15 and Ser78 phosphorylation of HSPB1 are enhanced by exogenous overexpression of human HSPB1 in murine cardiomyocytes undergoing oxidative stress, only Ser15 phosphorylation is suppressed by the mutation of Cys137 residue to Ser137 in HSPB1. In line with these findings, a phosphorylation mimic mutant of HSPB1 with the replacement of Ser15 to Asp15 showed lower oligomer stability and better protective ability against thermal aggregation in the Chinese hamster ovary cells.[54] Consequently, Cys137 residue is required for the Ser15 phosphorylation of HSPB1 that is more critical for the biological activities of HSPB1 than Ser78 and Ser82.

Once being phosphorylated, HSPB1 undergoes a conformational change from aggregated form to the dimer, thus more HSPB1 is found in the insoluble cytoskeletal fractions. Therefore, HSPB1 is also implicated in the regulation of cytoskeletal organization and maintenance of cytoskeletal integrity. It has been found that phosphorylation of HSPB1 facilitates the binding of residues surrounding the phosphosites to a compact multidomain region of actin-binding protein FLNC, and thus modulates its extension trajectory and promotes steered unfolding.[55] Under oxidative condition, more HSPB1 is found to the insoluble cytoskeletal fractions, which may facilitate HSPB1 to interact with client proteins. However, once Cys137 residue is replaced by Ser, HSPB1 fails to distribute to the insoluble cytoskeletal fractions; most HSPB1 still distributes in soluble cytosol fractions, indicating that oxidative stress-induced oxidation of Cys137 residue not only accounts for the phosphorylation of HSPB1 but also mediates subsequent interaction with client proteins in the cardiomyocytes. Given all this, next issue remaining to be addressed is about the downstream signaling following HSPB1 phosphorylation and redistribution.
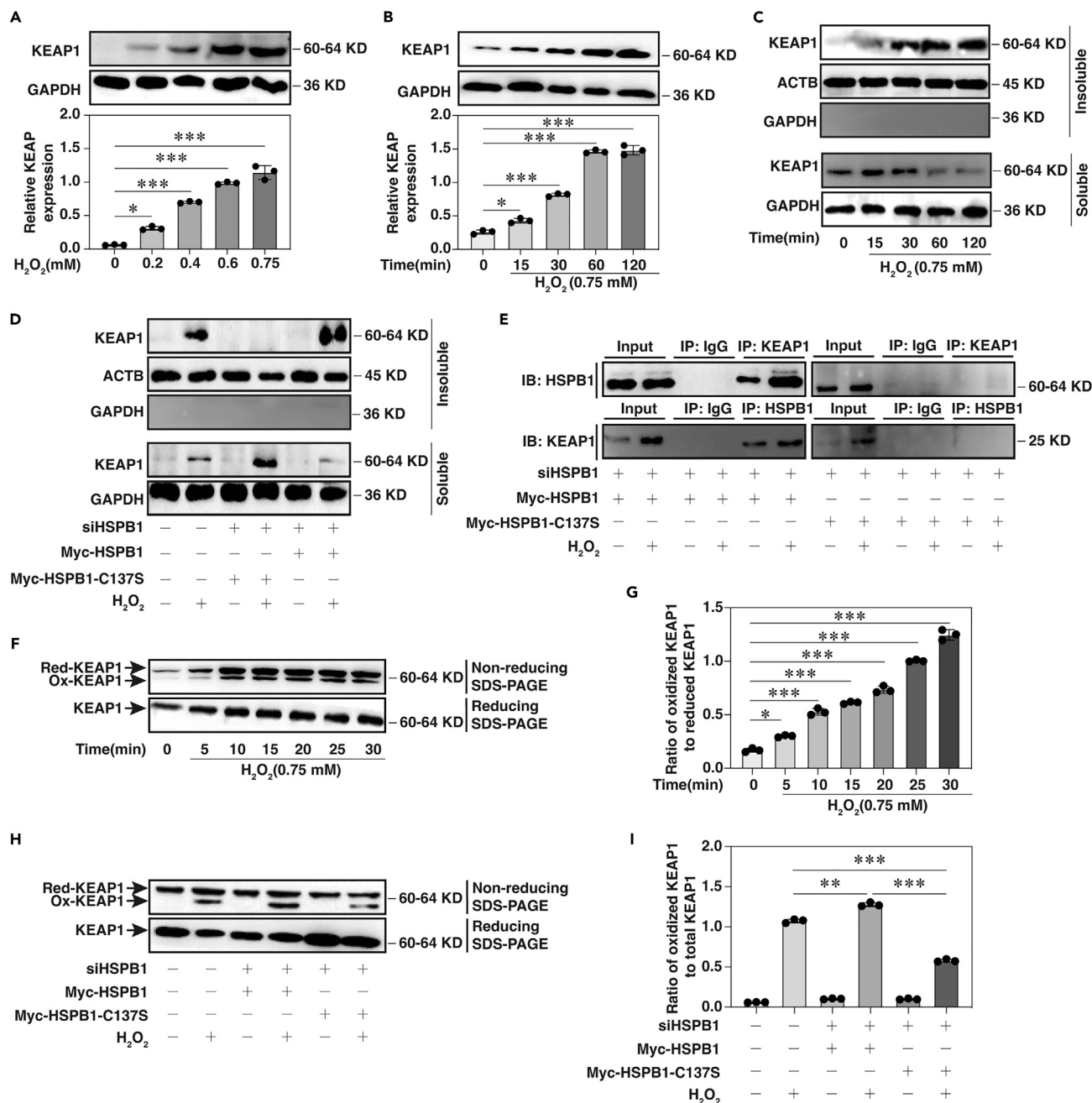
Figure 4. Mutation of HSPB1 in Cys137 blocked the binding of HSPB1 to KEAP1 and the oxidation of KEAP1

(A) H9c2 cells were treated by different doses of H_2O_2 for 60 min, the expression of KEAP1 was detected by reducing western blotting.

(B) H9c2 cells were treated by 0.75 mM H_2O_2 for different time, the expression of KEAP1 was detected by reducing western blotting.

(C) H9c2 cells were treated by different doses of H_2O_2 for 60 min, the expression of KEAP1 in the soluble and insoluble cellular components was detected by reducing western blotting.

(D) H9c2 cells were transfected HSPB1 siRNA for 24 h, and then transfected with pCMV-myc-HSPB1 or pCMV-myc-HSPB1 (C137S) for 48 h. Subsequently, cells were treated with 0.75 mM H_2O_2 for 120 min, the expression of KEAP1 in soluble and insoluble cell components was detected by reducing western blotting.

(E) H9c2 cells were transfected HSPB1 siRNA for 24 h, and then transfected with pCMV-myc-HSPB1 or pCMV-myc-HSPB1-C137S for 48 h. Subsequently, cells were treated with 0.75 mM H_2O_2 for 30 min, HSPB1-KEAP1 interaction was detected using Co-IP.

(F) H9c2 cells were treated by 0.75 mM H_2O_2 for different time, the expression of oxidized and reduced KEAP1 was detected by non-reducing western blotting, while the expression of total KEAP1 was determined by reducing western blotting.

(G) Accordingly, histogram showed the ratio of oxidized KEAP1 to reduced KEAP1 expression.

Figure 4. Continued

(H) H9c2 cells were transfected HSPB1 siRNA for 24 h, and then transfected with pCMV-myc-HSPB1 or pCMV-myc-HSPB1-C137S for 48 h. Subsequently, cells were treated with 0.75 mM H_2O_2 for 30 min, the expression of oxidized and reduced KEAP1 as well as total KEAP1 was detected as described above.

(I) Accordingly, histogram showed the ratio of oxidized KEAP1 to total KEAP1 expression. Measurement data were presented as mean $\pm$ SD. Differences among groups were determined by ANOVA and LSD-test or Student's t tests. *p < 0.05, **p < 0.01, ***p < 0.001.

NRF2, a nuclear transcriptional factor, functions as a master regulator of the antioxidant defense system against oxidative stress through transcriptional regulation of various genes and enzymes that function as antioxidants. Stabilization and translocation to the nucleus of NRF2 allows its transcriptional activity. Aberrant NRF2 expression and/or activity have been proved to be involved in the development of oxidative myocardial injury.[56,57] The transcriptional activity and protein stability of NRF2 is primarily controlled by its cytosolic inhibitor KEAP1, a cysteine-rich protein that serves as an adaptor of Cullin 3 (CUL3)-based E3 ligase. Under basal condition, KEAP1 binds to NRF2 and promotes its ubiquitination by the CUL3/RBX1 E3 ligase complex, and thereby targets it for proteasomal degradation. Under oxidative stress conditions, various stressful stimuli react with the critical cysteine residues of KEAP1, resulting in its conformational changes and subsequent release of NRF2. As such, NRF2 can translocate to nucleus, bind to the promoters of target genes, and exert its transcriptional regulatory activities.

While both HSPs and KEAP1/NFR2 signaling are considered as the master regulators of cellular homeostasis under stressful conditions, the crosstalk between these two systems has not been deeply investigated. It has been reported that HSP20 exerts protective roles against oxidative damages in the airway epithelial cells via activating NRF2/NAD(P)H quinone dehydrogenase 1 pathway. However, the role of KEAP1 in this signaling pathway has not been discussed.[26] In addition, KEAP1 not only regulates the expression of HSP90 in lipopolysaccharide-primed macrophages but also mediates HSP90 regulation of antioxidative pathway.[25] In this study, it is found that HSPB1 can bind to KEAP1 in cardiomyocytes undergoing oxidative stress, which may facilitate the release of NRF2 from KEAP1, and thus promotes the nuclear translocation of NRF2 and exerts antioxidant effect through regulating the transcription of NRF2-controlled antioxidant genes (*GCLM*, *HMOX1*, and *TXNRD1*). Cys137 residue is still indispensable for HSPB1 to interact with KEAP1 and subsequently regulates the nuclear translocation and transcriptional activity of NRF2.

In addition to KEAP1-dependent proteasomal degradation of NRF2, NRF2 is also regulated by two other E3 ubiquitin ligases: β-transducin repeat-containing protein and synoviolin 1. Although neither of these two E3 ubiquitin ligases is as substantial as KEAP1 for the degradation of NRF2, it is still of great importance to define whether KEAP1 is indispensable for HSPB1 to activate NRF2 in cardiomyocytes exposed to oxidative stress. Furthermore, SQSTM1, a critical autophagic adaptor, can interact with KEAP1 and result in its degradation through autophagy, thereby stabilizing and activating NRF2. NRF2 in turn induces SQSTM1 transcription through binding to the antioxidant response element in the promoter of SQSTM1.[19] This KEAP1/NRF2/SQSTM1 feedback loop is involved in oxidative stress-induced autophagy in the nucleus pulposus cells and protects intervertebral disc from degeneration.[58] Based on these findings, the role of SQSTM1 is also deserved to be identified in oxidative stress-induced activation of HSPB1/KEAP1/NRF2/ARE pathway.

In summary, for the first time, this study provides evidence that oxidative stress-induced homo-oxidized HSPB1 protects against cardiomyocyte injury via activation of KEAP1/NRF2 signaling pathway. Cys137 residue of HSPB1 is indispensable for maintaining its redox state and antioxidant activity as well as activating the downstream signaling cascade in cardiomyocytes undergoing oxidative stress (Figure 6). These findings not only broaden our insights into the antioxidant prosperity of HSPB1 but also improved our understanding of endogenous cardioprotective mechanisms underlying oxidative myocardial injury.

Limitations of the study

It is worthy to note that there are some limitations in this study. First, the exact roles of KEAP1 and NRF2 in homo-oxidized HSPB1-mediated protection against oxidative myocardial injury have not been identified through loss-of-function and rescue experiments, which is also of significance for defining the crosstalk between HSPB1 and KEAP1/NRF2 pathway and are full of challenges. Second, as mentioned previously, the role of KEAP1/NRF2/SQSTM1 feedback loop and KEAP1-independent activation of NRF2 may be also of great significance but remains unknown. Third, due to the cell diversity of cardiac tissues, *in vivo* studies have not been performed to confirm the findings from *in vitro* studies. Therefore, more attention will be paid to the previously mentioned deficiencies in our following studies.
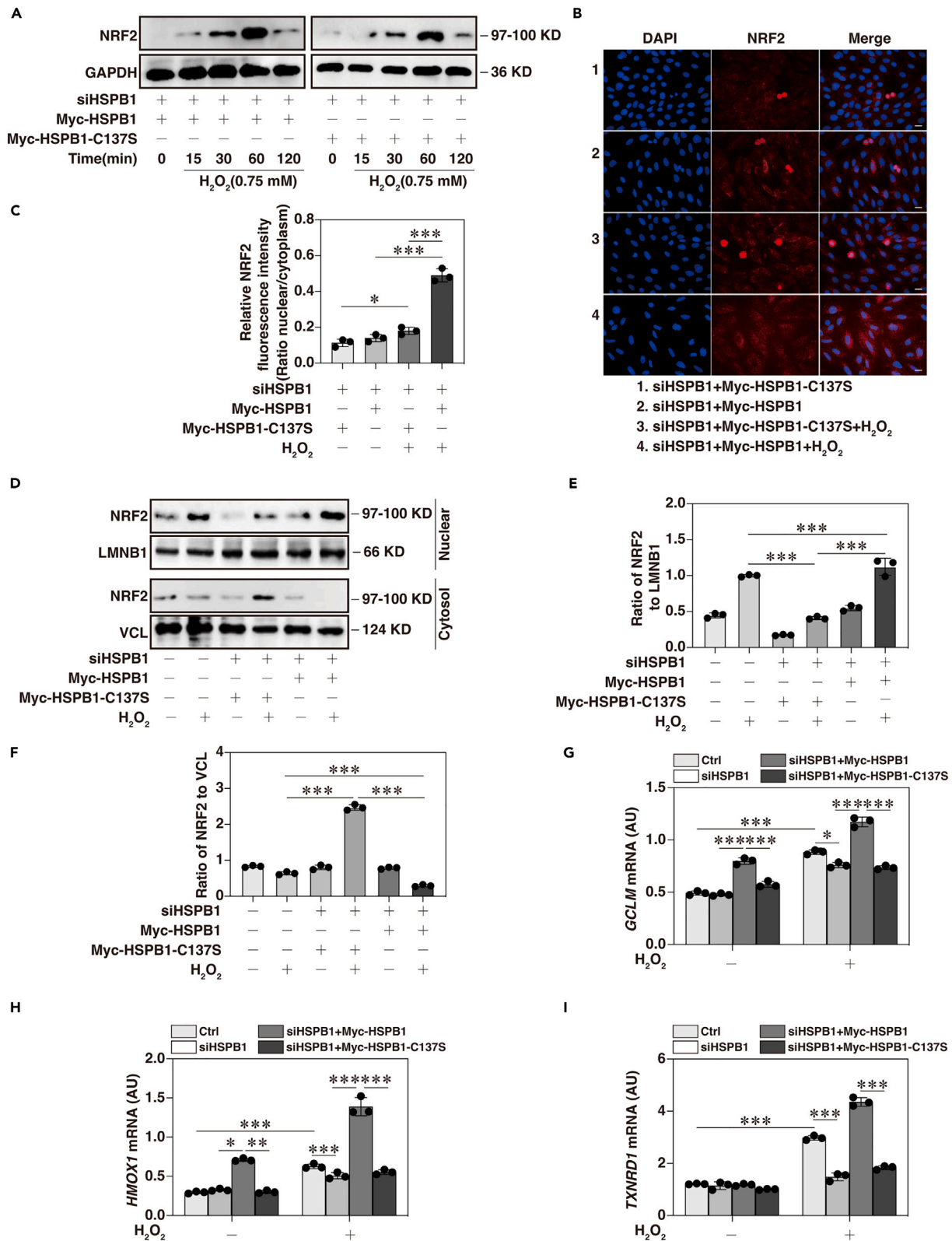
Figure 5. Mutation of HSPB1 in Cys137 dampened the activation of NRF2 following H$_2$O$_2$ challenge

H9c2 cells were transfected HSPB1 siRNA for 24 h, and then transfected with pCMV-myc-HSPB1 or pCMV-myc-HSPB1-C137S for 48 h.

(A) Subsequently, H9c2 cells were treated with 0.75 mM H$_2$O$_2$ for different time, the expression of NRF2 was detected by reducing western blotting.

(B) H9c2 cells were treated with 0.75 mM H$_2$O$_2$ for 60 min, the nuclear/cytoplasmic distribution of NRF2 was detected by reducing western blotting.

(C) Accordingly, histogram showed relative fluorescence intensity of NRF2 (ratio nuclear/cytoplasm).

(D) H9c2 cells were treated with 0.75 mM H$_2$O$_2$ for 60 min, the nuclear/cytoplasmic distribution of NRF2 was detected by immunofluorescence.

(E and F) Accordingly, histogram showed the ratio of NRF2 to LMNB1 expression (E) and the ratio of NRF2 to VCL expression (F).

(G–I) The mRNA expression of *GCLM* (G), *HMOX1* (H), and *TXNRD1* (I) *was detected by qPCR.* Measurement data were presented as mean $\pm$ SD. Differences among groups were determined by ANOVA and LSD-test or Student's t tests. *p < 0.05, **p < 0.01, ***p < 0.001.

STAR★METHODS

Detailed methods are provided in the online version of this paper and include the following:

- KEY RESOURCES TABLE
- RESOURCE AVAILABILITY
  - ○ Lead contact
  - ○ Materials availability
  - ○ Data and code availability
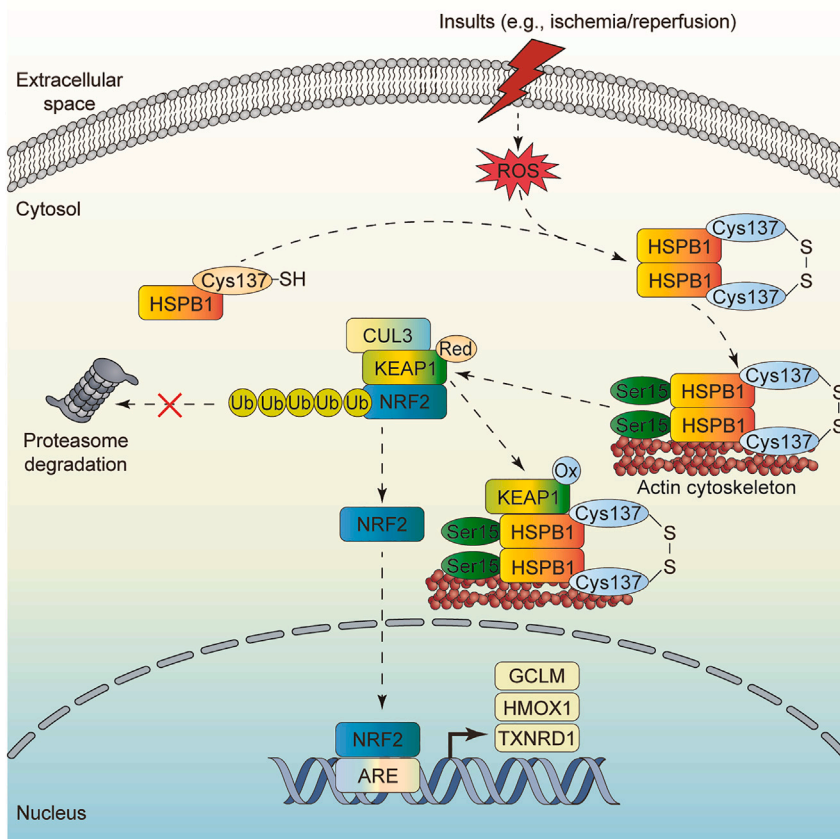- EXPERIMENTAL MODEL AND SUBJECT DETAILS

Figure 6. Schematic summary of the protective role of homo-oxidized HSPB1 against oxidative myocardial injury via activation of KEAP1/NRF2 signaling pathway

Following noxious insults (e.g., ischemia/reperfusion), excessive ROS generates and oxidizes redox sensitive cysteine residues (Cys137) on HSPB1, homo-oxidized HSPB1 forms in the cardiomyocytes, which in turn promotes its phosphorylation at Ser15 and distribution to insoluble actin components. Phosphorylated HSPB1 binds to KEAP1 and induces the oxidation of KEAP1, which facilitates the release of NRF2 from KEAP1, and thus promotes the nuclear translocation of NRF2 and exerts antioxidant effect through regulating the transcription of NRF2-controlled antioxidant genes (*GCLM*, *HMOX1*, and *TXNRD1*).

    ○ Cell line culture
    ○ Oxidative stress cell model
- METHOD DETAILS
    ○ siRNA, plasmid, and cell transfection
    ○ Cell fractionation
    ○ SDS-PAGE and immunoblotting
    ○ N-ethylmaleimide (NEM)-alkylated redox western-blotting
    ○ Quantitative reverse transcription polymerase chain reaction (qRT-PCR)
    ○ Immunofluorescence
    ○ Co-immunoprecipitation (Co-IP)
    ○ Cell viability assay
    ○ CASP3, CASP8, and CASP9 activity assay
    ○ Apoptosis analysis with flow cytometry
- QUANTIFICATION AND STATISTICAL ANALYSIS

SUPPLEMENTAL INFORMATION

Supplemental information can be found online at https://doi.org/10.1016/j.isci.2023.107443.

AUTHOR CONTRIBUTIONS

Conceptualization, H.Z. and K.W.; Methodology, N.W. and X.L.; Investigation, N.W., K.L., and X.L.; Writing – Original Draft, N.W.; Writing – Review & Editing, H.Z.; Funding Acquisition, H.Z., N.W., and K.W.; Supervision, H.Z. and K.W.

DECLARATION OF INTERESTS

The authors declare no competing interests.

INCLUSION AND DIVERSITY

We support inclusive, diverse, and equitable conduct of research.

REFERENCES

1. Anderson, J.L., and Morrow, D.A. (2017). Acute Myocardial Infarction. N. Engl. J. Med. *376*, 2053–2064. https://doi.org/10.1056/NEJMra1606915.

2. Khan, M.A., Hashim, M.J., Mustafa, H., Baniyas, M.Y., Al Suwaidi, S.K.B.M., AlKatheeri, R., Alblooshi, F.M.K., Almatrooshi, M.E.A.H., Alzaabi, M.E.H., Al Darmaki, R.S., and Lootah, S.N.A.H. (2020). Global Epidemiology of Ischemic Heart Disease: Results from the Global Burden of Disease Study. Cureus *12*, e9349. https://doi.org/10.7759/cureus.9349.

3. Vichova, T., and Motovska, Z. (2013). Oxidative stress: Predictive marker for coronary artery disease. Exp. Clin. Cardiol. *18*, e88–e91.

4. Kibel, A., Lukinac, A.M., Dambic, V., Juric, I., and Selthofer-Relatic, K. (2020). Oxidative Stress in Ischemic Heart Disease. Oxid. Med. Cell. Longev. *2020*, 6627144. https://doi.org/10.1155/2020/6627144.

5. Zitka, O., Skalickova, S., Gumulec, J., Masarik, M., Adam, V., Hubalek, J., Trnkova, L., Kruseova, J., Eckschlager, T., and Kizek, R. (2012). Redox status expressed as GSH:GSSG ratio as a marker for oxidative stress in paediatric tumour patients. Oncol. Lett. *4*, 1247–1253. https://doi.org/10.3892/ol.2012.931.

6. Kupatt, C., Hinkel, R., Horstkotte, J., Deiss, M., von Brühl, M.L., Bilzer, M., and Boekstegers, P. (2004). Selective retroinfusion of GSH and cariporide attenuates myocardial ischemia-reperfusion injury in a preclinical pig model. Cardiovasc. Res. *61*, 530–537. https://doi.org/10.1016/j.cardiores.2003.11.012.

7. Mirończuk-Chodakowska, I., Witkowska, A.M., and Zujko, M.E. (2018). Endogenous non-enzymatic antioxidants in the human body. Adv. Med. Sci. *63*, 68–78. https://doi.org/10.1016/j.advms.2017.05.005.

8. Reeg, S., Jung, T., Castro, J.P., Davies, K.J.A., Henze, A., and Grune, T. (2016). The molecular chaperone Hsp70 promotes the proteolytic removal of oxidatively damaged proteins by the proteasome. Free Radic. Biol. Med. *99*, 153–166. https://doi.org/10.1016/j.freeradbiomed.2016.08.002.

9. Song, N., Ma, J., Meng, X.W., Liu, H., Wang, H., Song, S.Y., Chen, Q.C., Liu, H.Y., Zhang, J., Peng, K., and Ji, F.H. (2020). Heat Shock Protein 70 Protects the Heart from Ischemia/Reperfusion Injury through Inhibition of p38 MAPK Signaling. Oxid. Med. Cell. Longev.

2020, 3908641. https://doi.org/10.1155/2020/3908641.

10. Wu, W., Lai, L., Xie, M., and Qiu, H. (2020). Insights of heat shock protein 22 in the cardiac protection against ischemic oxidative stress. Redox Biol. *34*, 101555. https://doi.org/10.1016/j.redox.2020.101555.

11. Islamovic, E., Duncan, A., Bers, D.M., Gerthoffer, W.T., and Mestril, R. (2007). Importance of small heat shock protein 20 (hsp20) C-terminal extension in cardioprotection. J. Mol. Cell. Cardiol. *42*, 862–869. https://doi.org/10.1016/j.yjmcc.2007.01.002.

12. Lutsch, G., Vetter, R., Offhauss, U., Wieske, M., Gröne, H.J., Klemenz, R., Schimke, I., Stahl, J., and Benndorf, R. (1997). Abundance and location of the small heat shock proteins HSP25 and alphaB-crystallin in rat and human heart. Circulation *96*, 3466–3476. https://doi.org/10.1161/01.cir.96.10.3466.

13. Liu, S., Li, J., Tao, Y., and Xiao, X. (2007). Small heat shock protein alphaB-crystallin binds to p53 to sequester its translocation to mitochondria during hydrogen peroxide-induced apoptosis. Biochem. Biophys. Res. Commun. *354*, 109–114. https://doi.org/10.1016/j.bbrc.2006.12.152.

14. Arrigo, A.P., Virot, S., Chaufour, S., Firdaus, W., Kretz-Remy, C., and Diaz-Latoud, C. (2005). Hsp27 consolidates intracellular redox homeostasis by upholding glutathione in its reduced form and by decreasing iron intracellular levels. Antioxid. Redox Signal. *7*, 414–422. https://doi.org/10.1089/ars.2005.7.414.

15. Liu, X., Liu, K., Li, C., Cai, J., Huang, L., Chen, H., Wang, H., Zou, J., Liu, M., Wang, K., et al. (2019). Heat-shock protein B1 upholds the cytoplasm reduced state to inhibit activation of the Hippo pathway in H9c2 cells. J. Cell. Physiol. *234*, 5117–5133. https://doi.org/10.1002/jcp.27322.

16. Arrigo, A.P. (2013). Human small heat shock proteins: protein interactomes of homo- and hetero-oligomeric complexes: an update. FEBS Lett. *587*, 1959–1969. https://doi.org/10.1016/j.febslet.2013.05.011.

17. Zavialov, A., Benndorf, R., Ehrnsperger, M., Zav'yalov, V., Dudich, I., Buchner, J., and Gaestel, M. (1998). The effect of the intersubunit disulfide bond on the structural and functional properties of the small heat shock protein Hsp25. Int. J. Biol. Macromol. *22*, 163–173. https://doi.org/10.1016/s0141-8130(98)00014-2.

18. Katsogiannou, M., Andrieu, C., and Rocchi, P. (2014). Heat shock protein 27 phosphorylation state is associated with cancer progression. Front. Genet. *5*, 346. https://doi.org/10.3389/fgene.2014.00346.

19. Lu, Y., An, L., Taylor, M.R.G., and Chen, Q.M. (2022). Nrf2 signaling in heart failure: expression of Nrf2, Keap1, antioxidant, and detoxification genes in dilated or ischemic cardiomyopathy. Physiol. Genom. *54*, 115–127. https://doi.org/10.1152/physiolgenomics.00079.2021.

20. Itoh, K., Wakabayashi, N., Katoh, Y., Ishii, T., Igarashi, K., Engel, J.D., and Yamamoto, M. (1999). Keap1 represses nuclear activation of antioxidant responsive elements by Nrf2 through binding to the amino-terminal Neh2 domain. Genes Dev. *13*, 76–86. https://doi.org/10.1101/gad.13.1.76.

21. Shanmugam, G., Challa, A.K., Litovsky, S.H., Devarajan, A., Wang, D., Jones, D.P., Darley-Usmar, V.M., and Rajasekaran, N.S. (2019). Enhanced Keap1-Nrf2 signaling protects the myocardium from isoproterenol-induced pathological remodeling in mice. Redox Biol. *27*, 101212. https://doi.org/10.1016/j.redox.2019.101212.

22. Zhang, H., Liu, Y., Cao, X., Wang, W., Cui, X., Yang, X., Wang, Y., and Shi, J. (2021). Nrf2 Promotes Inflammation in Early Myocardial Ischemia-Reperfusion via Recruitment and Activation of Macrophages. Front. Immunol. *12*, 763760. https://doi.org/10.3389/fimmu.2021.763760.

23. Jia, Y., Guo, H., Cheng, X., Zhang, Y., Si, M., Shi, J., and Ma, D. (2022). Hesperidin protects against cisplatin-induced cardiotoxicity in mice by regulating the p62-Keap1-Nrf2 pathway. Food Funct. *13*, 4205–4215. https://doi.org/10.1039/d2fo00298a.

24. Rinaldi Tosi, M.E., Bocanegra, V., Manucha, W., Gil Lorenzo, A., and Vallés, P.G. (2011). The Nrf2-Keap1 cellular defense pathway and heat shock protein 70 (Hsp70) response Role in protection against oxidative stress in early neonatal unilateral ureteral obstruction (UUO). Cell Stress Chaperones *16*, 57–68. https://doi.org/10.1007/s12192-010-0221-y.

25. Bonura, A., Giacomarra, M., and Montana, G. (2022). The Keap1 signaling in the regulation of HSP90 pathway. Cell Stress Chaperones *27*, 197–204. https://doi.org/10.1007/s12192-022-01253-5.

26. Bao, A., Ma, A., Zhang, H., Qiao, L., Ben, S., Zhou, X., and Zhang, M. (2020). Inducible expression of heat shock protein 20 protects airway epithelial cells against oxidative injury involving the Nrf2-NQO-1 pathway. Cell Biosci. *10*, 120. https://doi.org/10.1186/s13578-020-00483-3.

27. Aldini, G., Altomare, A., Baron, G., Vistoli, G., Carini, M., Borsani, L., and Sergio, F. (2018). N-Acetylcysteine as an antioxidant and disulphide breaking agent: the reasons why. Free Radic. Res. *52*, 751–762. https://doi.org/10.1080/10715762.2018.1468564.

28. Rajagopal, P., Liu, Y., Shi, L., Clouser, A.F., and Klevit, R.E. (2015). Structure of the alpha-crystallin domain from the redox-sensitive chaperone. J. Biomol. NMR *63*, 223–228. https://doi.org/10.1007/s10858-015-9973-0.

29. Pasupuleti, N., Gangadhariah, M., Padmanabha, S., Santhoshkumar, P., and Nagaraj, R.H. (2010). The role of the cysteine residue in the chaperone and anti-apoptotic functions of human Hsp27. J. Cell. Biochem. *110*, 408–419. https://doi.org/10.1002/jcb.22552.

30. Chalova, A.S., Sudnitsyna, M.V., Semenyuk, P.I., Orlov, V.N., and Gusev, N.B. (2014). Effect of disulfide crosslinking on thermal transitions

and chaperone-like activity of human small heat shock protein HspB1. Cell Stress Chaperones *19*, 963–972. https://doi.org/10.1007/s12192-014-0520-9.

31. Shimura, H., Miura-Shimura, Y., and Kosik, K.S. (2004). Binding of tau to heat shock protein 27 leads to decreased concentration of hyperphosphorylated tau and enhanced cell survival. J. Biol. Chem. *279*, 17957–17962. https://doi.org/10.1074/jbc.M400351200.

32. Matsumoto, T., Urushido, M., Ide, H., Ishihara, M., Hamada-Ode, K., Shimamura, Y., Ogata, K., Inoue, K., Taniguchi, Y., Taguchi, T., et al. (2015). Small Heat Shock Protein Beta-1 (HSPB1) Is Upregulated and Regulates Autophagy and Apoptosis of Renal Tubular Cells in Acute Kidney Injury. PLoS One *10*, e0126229. https://doi.org/10.1371/journal.pone.0126229.

33. Kato, K., Hasegawa, K., Goto, S., and Inaguma, Y. (1994). Dissociation as a result of phosphorylation of an aggregated form of the small stress protein, hsp27. J. Biol. Chem. *269*, 11274–11278.

34. Lambert, H., Charette, S.J., Bernier, A.F., Guimond, A., and Landry, J. (1999). HSP27 multimerization mediated by phosphorylation-sensitive intermolecular interactions at the amino terminus. J. Biol. Chem. *274*, 9378–9385. https://doi.org/10.1074/jbc.274.14.9378.

35. Clarke, J.P., and Mearow, K.M. (2013). Cell stress promotes the association of phosphorylated HspB1 with F-actin. PLoS One *8*, e68978. https://doi.org/10.1371/journal.pone.0068978.

36. Kostenko, S., and Moens, U. (2009). Heat shock protein 27 phosphorylation: kinases, phosphatases, functions and pathology. Cell. Mol. Life Sci. *66*, 3289–3307. https://doi.org/10.1007/s00018-009-0086-3.

37. Landry, J., Lambert, H., Zhou, M., Lavoie, J.N., Hickey, E., Weber, L.A., and Anderson, C.W. (1992). Human HSP27 is phosphorylated at serines 78 and 82 by heat shock and mitogen-activated kinases that recognize the same amino acid motif as S6 kinase II. J. Biol. Chem. *267*, 794–803.

38. Hayes, D., Napoli, V., Mazurkie, A., Stafford, W.F., and Graceffa, P. (2009). Phosphorylation dependence of hsp27 multimeric size and molecular chaperone function. J. Biol. Chem. *284*, 18801–18807. https://doi.org/10.1074/jbc.M109.011353.

39. McMahon, M., Itoh, K., Yamamoto, M., and Hayes, J.D. (2003). Keap1-dependent proteasomal degradation of transcription factor Nrf2 contributes to the negative regulation of antioxidant response element-driven gene expression. J. Biol. Chem. *278*, 21592–21600. https://doi.org/10.1074/jbc.M300931200.

40. Kehm, R., Baldensperger, T., Raupbach, J., and Höhn, A. (2021). Protein oxidation - Formation mechanisms, detection and relevance as biomarkers in human diseases. Redox Biol. *42*, 101901. https://doi.org/10.1016/j.redox.2021.101901.

41. Celi, P., and Gabai, G. (2015). Oxidant/ Antioxidant Balance in Animal Nutrition and Health: The Role of Protein Oxidation. Front. Vet. Sci. *2*, 48. https://doi.org/10.3389/fvets. 2015.00048.

42. Suh, S.K., Hood, B.L., Kim, B.J., Conrads, T.P., Veenstra, T.D., and Song, B.J. (2004). Identification of oxidized mitochondrial proteins in alcohol-exposed human hepatoma cells and mouse liver. Proteomics *4*, 3401–3412. https://doi.org/10.1002/pmic. 200400971.

43. Lin, C.Y., Hu, C.T., Cheng, C.C., Lee, M.C., Pan, S.M., Lin, T.Y., and Wu, W.S. (2016). Oxidation of heat shock protein 60 and protein disulfide isomerase activates ERK and migration of human hepatocellular carcinoma HepG2. Oncotarget *7*, 11067– 11082. https://doi.org/10.18632/ oncotarget.7093.

44. Grunwald, M.S., Pires, A.S., Zanotto-Filho, A., Gasparotto, J., Gelain, D.P., Demartini, D.R., Schöler, C.M., de Bittencourt, P.I.H., Jr., and Moreira, J.C.F. (2014). The oxidation of HSP70 is associated with functional impairment and lack of stimulatory capacity. Cell Stress Chaperones *19*, 913–925. https://doi.org/10. 1007/s12192-014-0516-5.

45. Liu, L., Zhang, X.J., Jiang, S.R., Ding, Z.N., Ding, G.X., Huang, J., and Cheng, Y.L. (2007). Heat shock protein 27 regulates oxidative stress-induced apoptosis in cardiomyocytes: mechanisms via reactive oxygen species generation and Akt activation. Chin. Med. J. *120*, 2271–2277.

46. Boelens, W.C. (2020). Structural aspects of the human small heat shock proteins related to their functional activities. Cell Stress Chaperones *25*, 581–591. https://doi.org/10. 1007/s12192-020-01093-1.

47. Diaz-Latoud, C., Buache, E., Javouhey, E., and Arrigo, A.P. (2005). Substitution of the unique cysteine residue of murine Hsp25 interferes with the protective activity of this stress protein through inhibition of dimer formation. Antioxid. Redox Signal. *7*, 436–445. https://doi.org/10.1089/ars.2005. 7.436.

48. Mymrikov, E.V., Seit-Nebi, A.S., and Gusev, N.B. (2012). Heterooligomeric complexes of human small heat shock proteins. Cell Stress Chaperones *17*, 157–169. https://doi.org/10. 1007/s12192-011-0296-0.

49. Alderson, T.R., Roche, J., Gastall, H.Y., Dias, D.M., Pritišanac, I., Ying, J., Bax, A., Benesch, J.L.P., and Baldwin, A.J. (2019). Local unfolding of the HSP27 monomer regulates chaperone activity. Nat. Commun. *10*, 1068. https://doi.org/10.1038/s41467-019-08557-8.

50. Bruey, J.M., Ducasse, C., Bonniaud, P., Ravagnan, L., Susin, S.A., Diaz-Latoud, C., Gurbuxani, S., Arrigo, A.P., Kroemer, G., Solary, E., and Garrido, C. (2000). Hsp27 negatively regulates cell death by interacting with cytochrome c. Nat. Cell Biol. *2*, 645–652. https://doi.org/10.1038/35023595.

51. Arrigo, A.P. (2017). Mammalian HspB1 (Hsp27) is a molecular sensor linked to the physiology and environment of the cell. Cell Stress Chaperones *22*, 517–529. https://doi. org/10.1007/s12192-017-0765-1.

52. Arrigo, A.P. (2018). Analysis of HspB1 (Hsp27) Oligomerization and Phosphorylation Patterns and Its Interaction with Specific Client Polypeptides. Methods Mol. Biol. *1709*, 163–178. https://doi.org/10.1007/978- 1-4939-7477-1_12.

53. Gusev, N.B., Bogatcheva, N.V., and Marston, S.B. (2002). Structure and properties of small heat shock proteins (sHsp) and their interaction with cytoskeleton proteins. Biochemistry *67*, 511–519. https://doi.org/10. 1023/a:1015549725819.

54. Sha, E., Nakamura, M., Ankai, K., Yamamoto, Y.Y., Oka, T., and Yohda, M. (2019). Functional and structural characterization of HspB1/ Hsp27 from Chinese hamster ovary cells. FEBS Open Bio *9*, 1826–1834. https://doi. org/10.1002/2211-5463.12726.

55. Collier, M.P., Alderson, T.R., de Villiers, C.P., Nicholls, D., Gastall, H.Y., Allison, T.M., Degiacomi, M.T., Jiang, H., Mlynek, G., Fürst, D.O., et al. (2019). HspB1 phosphorylation regulates its intramolecular dynamics and mechanosensitive molecular chaperone interaction with filamin C. Sci. Adv. *5*, eaav8421. https://doi.org/10.1126/sciadv. aav8421.

56. Ruotsalainen, A.K., Inkala, M., Partanen, M.E., Lappalainen, J.P., Kansanen, E., Mäkinen, P.I., Heinonen, S.E., Laitinen, H.M., Heikkilä, J., Vatanen, T., et al. (2013). The absence of macrophage Nrf2 promotes early atherogenesis. Cardiovasc. Res. *98*, 107–115. https://doi.org/10.1093/cvr/cvt008.

57. Ichikawa, T., Li, J., Meyer, C.J., Janicki, J.S., Hannink, M., and Cui, T. (2009). Dihydro- CDDO-trifluoroethyl amide (dh404), a novel Nrf2 activator, suppresses oxidative stress in cardiomyocytes. PLoS One *4*, e8391. https:// doi.org/10.1371/journal.pone.0008391.

58. Tang, Z., Hu, B., Zang, F., Wang, J., Zhang, X., and Chen, H. (2019). Nrf2 drives oxidative stress-induced autophagy in nucleus pulposus cells via a Keap1/Nrf2/p62 feedback loop to protect intervertebral disc from degeneration. Cell Death Dis. *10*, 510. https://doi.org/10.1038/s41419-019-1701-3.

59. Liu, X., Wang, L., Cai, J., Liu, K., Liu, M., Wang, H., and Zhang, H. (2019). N-acetylcysteine alleviates H2O2-induced damage via regulating the redox status of intracellular antioxidants in H9c2 cells. Int. J. Mol. Med. *43*, 199–208. https://doi.org/10.3892/ijmm. 2018.3962.

STAR★METHODS

KEY RESOURCES TABLE

REAGENT or RESOURCE	SOURCE	IDENTIFIER
Antibodies		
MYC	Cell Signaling Technology	5605 RRID: AB_1903938
phospho-HSPB1 (Ser82)	Cell Signaling Technology	2401 RRID: AB_331644
phospho-HSP27 (Ser15)	Cell Signaling Technology	2404 RRID: AB_330738
KEAP1	Cell Signaling Technology	4678 RRID: AB_10548196
NRF2	Cell Signaling Technology	33649 RRID: AB_2922991
GAPDH	Cell Signaling Technology	2118 RRID: AB_561053
ACTB	Cell Signaling Technology	3700 RRID: AB_2242334
HSPB1	Enzo Life Sciences	ADI-SPA-801-D RRID: AB_2039212
HSPB1	Santa Cruz biotechnology	sc-1049 RRID: AB_631674
Chemicals, peptides, and recombinant proteins		
N-acetylcysteine	Sigma-Aldrich	A9165
N-ethylmaleimide	Sigma-Aldrich	E3876
hydrogen peroxide	Sigma-Aldrich	323381
trichloroacetic acid	Sigma-Aldrich	T0699
Critical commercial assays		
3-(4,5-dimethylthiazol-2-yl)-2,5-diphenyl tetrazolium bromide (MTT) assay	Beyotime Biotechnology	C0009S
CASP3 activity assay	BioVision	K106
CASP8 activity assay	BioVision	K113
CASP9 activity assay	BioVision	K119
Annexin V-FITC/propidium iodide (PI) double staining apoptosis assay kit	BD Pharmingen	556547
Bicinchoninic acid protein assay kit	Thermo Fisher Scientific	23227
Experimental models: Cell lines		
H9c2	ATCC	CRL-1446
Oligonucleotides		
siHSPB1: 5′-CCGCUGCCCAAAGCAG UCACACAAU-3′	Thermo Fisher Scientific	315499E09
Rat *TXNRD1* primer_F	This study	GGATTCCTGGCTGGTATCGG
Rat *TXNRD1* primer_R	This study	TTGTGGACTTAGCGGTCACC
Rat *GC1M* primer_F	This study	TTAGTTCAGAGCAAGAAGATTGT
Rat *GC1M* primer_R	This study	TTACTATTGGGTTTTACCTGTGCC
Rat *HMOX1* primer_F	This study	CTCATCCTGAGCTGCTGGTG
Rat *HMOX1* primer_R	This study	GATGCTCGGGAAGGTGAAAA
Rat *GAPDH* primer_F	This study	CCATCAACGACCCCTTCATT
Rat *GAPDH* primer_R	This study	CACGACATACTCAGCACCAGC
Recombinant DNA		
Human pCMV-Myc-HSPB1	This study	N/A
Human pCMV-HA-HSPB1	This study	N/A

Continued

REAGENT or RESOURCE	SOURCE	IDENTIFIER
Human pCMV-Myc-HSPB1-C137S	This study	N/A
Software and algorithms		
Image Lab software version 6.1	Bio-Rad	http://www.bio-rad.com/en-us/product/image-lab-software?ID=KRE6P5E8Z
CFX Manager software version 3.1	Bio-Rad	http://www.bio-rad.com/en-us/sku/1845000-cfx-manager-software?ID=1845000
GraphPad Prism 8	GraphPad Software	https://www.graphpad.com/scientific-software/prism/

RESOURCE AVAILABILITY

Lead contact

Further information and requests for reagents may be directed to, and will be fulfilled upon reasonable request by, the lead contact Huali Zhang (zhanghuali@csu.edu.cn).

Materials availability

All unique reagents generated in this study are available upon reasonable request from the lead contact.

Data and code availability

- All datasets generated or analyzed during this study are included in the published article and will be shared by the lead contact upon reasonable request.

- This paper does not report original code.

- Any additional information required to reanalyze the data reported in this paper is available from the lead contact upon reasonable request.

EXPERIMENTAL MODEL AND SUBJECT DETAILS

Cell line culture

Rat H9c2 cardiomyocyte cell line was obtained from American Type Culture Collection (#CRL-1446, Manassas, VA, USA) and cultured in the Dulbecco's modified Eagle's medium (DMEM) supplemented with 10% fetal bovine serum (Gibco; Thermo Fisher Scientific, Inc., Waltham, MA, USA), 100 µg/mL streptomycin, and 100 U/mL penicillin. Cells were routinely maintained at 37°C under a humidified atmosphere containing 5% CO_2. After reaching confluence, cells were trypsinized, resuspended in DMEM, and then seeded in a 6-well plate 24 h prior to the treatment.

Oxidative stress cell model

Rat H9c2 cardiomyocytes was seeded in a 6-well plate. After the cells adhered, the supernatant was removed, washed twice with PBS. Then, DMEM medium with different concentration of H_2O_2 (0.2, 0.4, 0.75, and 1 mM) was added and stimulated for 30min. Then H9c2 cardiomyocytes were treated by 0.75 mM H_2O_2 for different time (15, 30, 60, 90, 120 min).

METHOD DETAILS

siRNA, plasmid, and cell transfection

The specific siRNA against HSPB1 (siHSPB1) and scrambled siRNA were purchased from Thermo Fisher Scientific, Inc. (#315499E09, Waltham, MA, USA). The sense strand of siHSPB1 was: 5'-CCGCUGCCCAAAG CAGUCACACAAU-3'. Human pCMV-Myc-HSPB1, pCMV-HA-HSPB1, and pCMV-Myc-HSPB1-C137S plasmids were constructed by our lab and identified through complete plasmid DNA sequencing. H9c2 cells were seeded in six-well plates at a density of 1 × 10^5 cells/well and allowed to reach approximately 50% confluence on the day of transfection. Cells were transfected with 30 pmol/well siHSPB1 using Lipofectamine RNAiMax reagent (Thermo Fisher Scientific, #13778030, Waltham, MA, USA) according to the manufacturer's instructions. At 24 h after transfection, the cells were co-transfected with 2 µg of

pCMV-Myc-HSPB1, pCMV-HA-HSPB1, or pCMV-Myc-HSPB1-C137S plasmid using MegaTran 1.0 (OriGene Technologies, #TT200004, Rockville, MD, USA) for 48h.

Cell fractionation

To separate total cellular protein into a soluable and insoluable cell fractions, rat H9c2 cardiomyocytes were lysed in ice-cold Triton lysis buffer containing 1% TritonX-100, 0.5M ethylene diamine tetraacetic acid (EDTA), 150 mM sodium chloride, and 1M Tris-Hcl (PH 7.4). The homogenate was then centrifuged at 12,000×g for 10 min at 4°C, the supernatants containing TritonX™-100 soluble fractions were collected. The precipitates were washed by Triton lysis buffer twice and then lysed in sodium dodecyl sulfate (SDS) lysis buffer containing 1% SDS, 10mM EDTA and 50mM Tris (pH 8.0). The homogenate was then centrifuged at 12,000×g for 10 min at 4°C, the supernatants containing insoluble fractions were collected. The cytoplasmic and nuclear fractions of rat H9c2 cardiomyocytes were separated using a nuclear and cytoplasmic protein extraction kit (Beyotime Biotechnology, #P0027, Shanghai, China) according to the manufacturer's protocols.

SDS-PAGE and immunoblotting

Rat H9c2 cardiomyocytes were lysed in SDS lysis buffer (50mM Tris-HCl, pH 8.1; 1% SDS, 10 mM EDTA, PH 8.0) with proteinase inhibitor cocktail (Roche, #11836170001, Basel, Switzerland). The homogenate was then centrifuged at 12,000×g for 10 min (4°C) and the protein concentrations of supernatants were determined using a bicinchoninic acid protein assay kit (Thermo Fisher Scientific, Inc., #23227, Waltham, MA, USA). 30 ∼ 50 μg protein was loaded onto 12% SDS-PAGE gels and then transferred onto polyvinylidene fluoride membranes (Millipore, Billerica, MA, USA). After blocking with 5% non-fat milk in Tris-buffered saline with Tween 20, membranes were incubated with different primary antibodies (dilution: 1:1000) at 4°C overnight, followed by HRP-conjugated secondary antibody (dilution: 1:5000) at room temperature for 1 h. GAPDH was used as a loading control for protein normalization. Enhanced chemiluminescence (ECL) was performed using Clarity Max™ Western ECL Substrates (Bio-Rad, Inc., #1705062, Hercules, CA, USA). The relative band intensity was analyzed by the ImageJ software (NIH, Bethesda, MD, United States).

N-ethylmaleimide (NEM)-alkylated redox western-blotting

NEM-alkylated redox Western-blotting was performed to detect the redox status of HSPB1 and KEAP1 as we previously reported.[59] After treatment, rat H9c2 cardiomyocytes were washed twice with ice-cold phosphate buffer saline (PBS) and then precipitated with chilled 10% trichloroacetic acid for 30 min at 4°C. The homogenate was then centrifuged at 12,000×g for 10 min (4°C), the harvested protein pellets were washed twice with 100% acetone and dissolved in nonreducing buffer (100mM Tris-HCl, pH6.8; 2% SDS; and 40 mM NEM), and 5% dithiothreitol was added to the samples. 30 ∼ 50 μg protein was loaded onto a non-reducing SDS-PAGE gels and the proteins were transferred onto polyvinylidene fluoride membranes (Millipore, Billerica, MA, USA). After blocking with 5% non-fat milk in Tris-buffered saline with Tween 20, membranes were incubated with different primary antibodies (dilution: 1:1000) at 4°C overnight, followed by HRP-conjugated secondary antibody (dilution: 1:5000) at room temperature for 1 h. Enhanced chemiluminescence (ECL) was performed using Clarity Max™ Western ECL Substrates (Bio-Rad, Inc., #1705062, Hercules, CA, USA). The relative band intensity was analyzed by Quantity One software (Bio-Rad, Inc., Hercules, CA, United States).

Quantitative reverse transcription polymerase chain reaction (qRT-PCR)

Total RNA from rat H9c2 cardiomyocytes was extracted using TRIzol™ reagent (Thermo Fisher Scientific, Inc., #15596026, Waltham, MA, USA) and reverse transcribed to cDNA with a LiPrimeScript™ RT reagent Kit with gDNA Eraser (Takara shuzo Co., #RR047B, Kyoto, Japan). The SYBR Green Master Mix: SYBR Premix Ex Taq II (Takara Shuzo Co., #RR820A, Kyoto, Japan) was used for qPCR to detect the expression of related genes using an ABI 7500 real-time PCR system (Life Technology Corporation, Carlsbad, CA). Gene expression was analyzed using the equation Ratio = $2^{-\triangle\triangle Ct}$ and was normalized by glyceraldehyde-3-phosphate dehydrogenase (GAPDH).

Immunofluorescence

After treatment, rat H9c2 cardiomyocytes were washed with PBS for three times and fixed with 4% paraformaldehyde for 10 min. Subsequently, they were washed with pre-cooled PBS for 15 min and permeabilized with 0.5% Triton™ X-100 dissolved in PBS (Beijing Dingguo Changsheng Biotechnology

Co., Ltd., #AR-0341, Beijing, China) for 15 min. After incubating with 5% bovine serum albumin for 30 min at room temperature, cells were incubated with primary antibodies at 4°C overnight, followed by incubation with the secondary antibody at 37°C for 1 h. Fluorescent images were captured using a fluorescence microscope (OLYMPUS, #BX53, Tokyo, Japan).

Co-immunoprecipitation (Co-IP)

Rat H9c2 cardiomyocytes were lysed in a lysis buffer containing 20 mM Tris-HCl [pH 7.5], 150 mM NaCl, 5 mM EDTA, 1% NP-40, together with proteinase inhibitor cocktail and were left on ice for 30 min. The homogenate was then centrifuged at 12,000×g for 10 min (4°C) and the protein concentrations of supernatants were determined using a bicinchoninic acid protein assay kit (Thermo Fisher Scientific, Inc., #23227, Waltham, MA, USA). 500 µg protein was incubated together with the desired antibody or IgG antibody (1:50) at 4°C overnight, followed by incubation with pre-cleared PureProteome™ Protein A Magnetic Bead (Millipore, #LSKMAGA10, Billerica, MA, USA) for 15min ∼ 1h at room temperature with constant rotation. The lysate-beads mixture was centrifuged at 300 g for 5 min at 4°C. The beads were resuspended with SDS lysis buffer, and proteins were eluted from beads through boiling for 5 min at 95°C and further loaded on the SDS-PAGE gel and analyzed by immunoblotting as described above.

Cell viability assay

Cell viability was measured using a 3-(4,5-dimethylthiazol-2-yl)-2,5-diphenyl tetrazolium bromide (MTT) assay (Beyotime Biotechnology, # C0009S, Shanghai, China). Briefly, H9c2 cells (5×10^3/well) were seeded in 96-well culture plates. After treatment, the culture medium was replaced with 200 µL/well of MTT solution (5 mg/mL stock solution in PBS, diluted with culture medium to the final concentration of 0.5 mg/mL). After a 4-hour incubation at 37°C, the solution was removed, and the formazan was solubilized in 150 µL of dimethyl sulfoxide. The absorbance was measured at 570 nm using an automated microplate reader (Bio-Tek Instruments, Inc., #ELX-800, Winooski, VT, USA). Cell viability was calculated by normalizing the control cells to have 100% viability.

CASP3, CASP8, and CASP9 activity assay

Caspase-3, -8 and -9 activities were measured using Caspase-3 (#K106), caspase-8 (#K113), and caspase-9 (#K119) assay kits from BioVision, Inc. (Milpitas, CA, USA). After treatment, cellular proteins were extracted by using cell lysis buffer and then quantified using a bicinchoninic acid protein assay kit (Thermo Fisher Scientific, Inc., #23227, Waltham, MA, USA). Subsequently, 150 ∼ 200 ug cellular proteins were reacted with corresponding substrates (DEVD-pNA, IETD-pNA and LEHD-pNA). Caspase-3, -8 and -9 activities were subsequently measured as the optical density of the cleaved substrate at 405 nm using a microplate reader (Bio-Tek Instruments, Inc., #ELX-800, Winooski, VT, USA).

Apoptosis analysis with flow cytometry

Cell apoptosis was detected by staining using an Annexin V-FITC/propidium iodide (PI) double staining apoptosis assay kit (BD Pharmingen™, #556547, San Diego, CA USA) according to the manufacturer's instructions. Briefly, cells were harvested after treatment and resuspended in binding buffer. Aliquots of 1×10^5 cells were then mixed with annexin V-FITC and PI solution for 15 min at room temperature in the dark. After incubation, 400 µL binding buffer was added, and cells were suspended with binding buffer and analyzed by flow cytometer (Becton Dickinson). Cell population in the lower right quadrant (Annexin V+/PI-) represents the early apoptotic cells, and population in the upper right quadrant (Annexin V+/PI+) represents the late apoptotic or dead cells. The sum of the early and late apoptotic rates was considered as the total apoptotic rate.

QUANTIFICATION AND STATISTICAL ANALYSIS

All statistical analyses were performed using GraphPad Prism 8.0 software. The measurement data were represented as mean $\pm$ standard deviation (SD). The means of two groups were compared using unpaired Student's t-tests. Analysis of variance (ANOVA) was used to test for differences among three or more groups, and if the ANOVA showed significant differences, we used Tukey's post-hoc test to identify pairs with significant differences. A two-tailed P-value <0.05 was considered statistically significant. In this study, an electronic laboratory notebook was not used.